Supplemental information

Anion transport in biologically relevant lipid mixtures

Krystyna Maslowska-Jarzyna,[a,b] Sarah Rooijmans,[a,c] Daniel A. McNaughton,[a] William G. Ryder,[d] Edward York,[a] Moniek Tromp[c] and Philip A. Gale[a,*]

[a] School of Mathematical and Physical Sciences, University of Technology Sydney, Sydney, NSW 2007, Australia.
[b] Faculty of Chemistry, Biological and Chemical Research Centre, University of Warsaw, Żwirki i Wigury 101, Warsaw, Poland.
[c] Materials Chemistry – Zernike Institute for Advanced Materials, University of Groningen Nijenborgh 4, 9747 AG Groningen, The Netherlands.
[d] School of Chemistry, The University of Sydney, Sydney, NSW 2006, Australia.

*E-mail: philip.gale@uts.edu.au

Contents

1 General information

1.1 Materials

All chemicals and solvents were of reagent grade (>95%) and purchased from commercial supplies without further purification, unless otherwise noted. 4-(Trifluoromethyl)aniline, 3,4-diethoxy-3-cyclobutene-1,2-dione and zinc trifluoromethanesulfonate were purchased from Sigma Aldrich. Deuterated solvent was purchased from Cambridge Isotope Laboratories. Palmitoyl-2-oleoyl-*sn*-glycero-3-phosphocholine (POPC), palmitoyl-2-oleoyl-*sn*-glycero-3-phosphoethanolamine (POPE) and 1,2-dipalmitoyl-*sn*-glycero-3-phospho-L-serine (PS) were purchased from Avanti Polar Lipids. *N*-palmitoyl-D-sphingomyelin, cardiolipin and cholesterol were purchased from Sigma-Aldrich. L-α-phosphatidylinositol was purchased from MilliporeSigma. Deionised water was collected from a Merck Millipore Milli-Q™ reference ultrapure water purification system.

1.2 Instruments and methods

The ISE assay experiments were conducted on the Fisherbrand™ Accumet™ Chloride Combination Electrode, and fluorescence-based transport data was recorded on an Agilent Cary Eclipse Fluorescence spectrometer, equipped with a PCB 1500 Water Peltier temperature control system and an Agilent Technologies Thermostatted Multicell Holder with stirring.

2 Synthetic procedures

2.1 3,4-Bis(4-(trifluoromethyl)phenylamino)cyclobut-3-ene-1,2-dione **1**

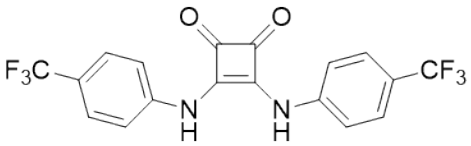

1

Compound **1** was synthesized following the method developed by Rostami et al.[1]

4-(Trifluoromethyl)aniline (783 µL, 6.29 mmol, 2.1 eqv) was added to a solution of 3,4-diethoxy-3-cyclobutene-1,2-dione (0.5 g, 2.94 mmol, 1 eqv) and zinc trifluoromethanesulfonate (210 mg, 0.58 mmol, 20 mol%) in 19:1 toluene:DMF (5 mL). The reaction was heated overnight at 100 °C. After cooling, a precipitate was formed, filtered off and washed with methanol until the filtrate appeared colourless. The resulting solid was dried in high vacuum for 24 hours and compound **1** was obtained as a pale-yellow solid (0.88 g, 2.20 mmol, 75%). Characterization was consistent with reported values.[2] ^{1}H NMR (300 MHz, DMSO-d_6) δ = 7.63 (td J=8.7 Hz, 4H), 7.74 (d, J=8.7 Hz, 4H), 10.26 (br. s, 2H; NH); LRMS(ESI-): m/z: 399.1 $[M-H]^-$.

[1] A. Rostami, A. Colin, X. Y. Li, M. G. Chudzinski, A. J. Lough, M. S. Taylor, *J. Org. Chem*., **2010**, *75*, 3983–3992.
[2] N. Busschaert, I. L. Kirby, S. Young, S. J. Coles, P. N. Horton, M. E. Light, P. A. Gale, *Angew. Chem*., **2012**, *51*, 4426–4430.

3 Selection of lipids

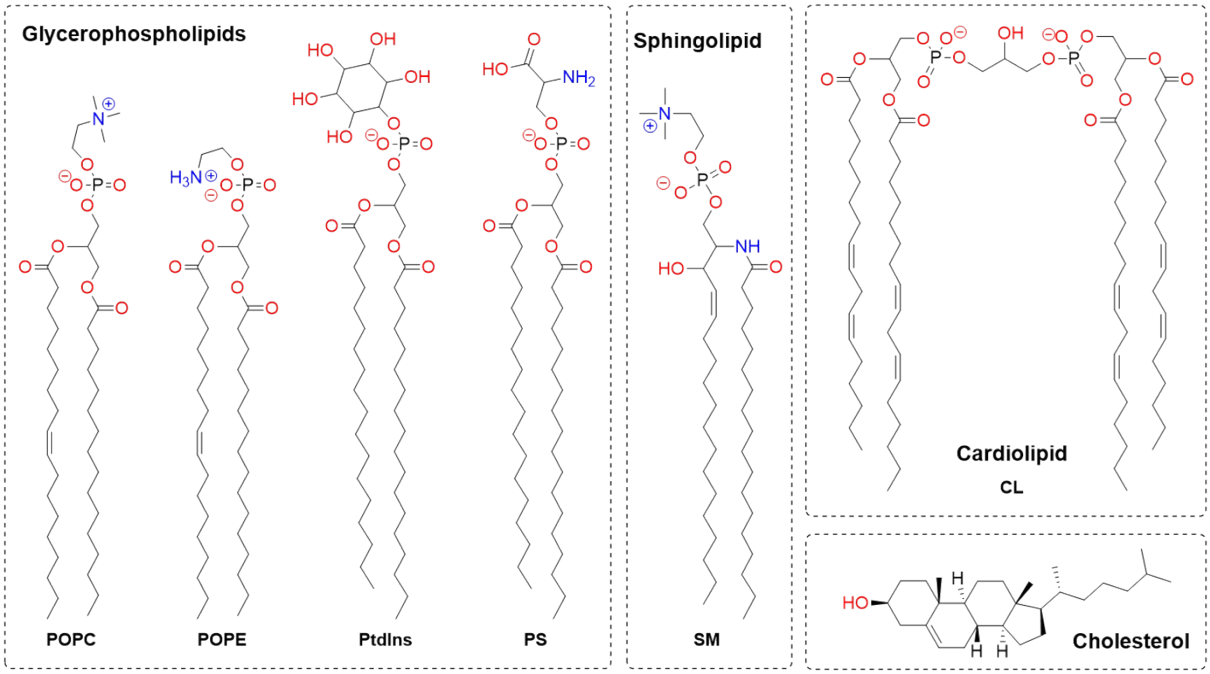

Figure S1. Chemical structures of the various lipids used when constructing the organelle mimicking vesicles. Palmitoyl-2-oleoyl-*sn*-glycero-3-phosphocholine (POPC), palmitoyl-2-oleoyl-*sn*-glycero-3-phosphoethanolamine (POPE), L-α-phosphatidylinositol (PtdIns), 1,2-dipalmitoyl-*sn*-glycero-3-phospho-L-serine (PS), *N*-palmitoyl-D-sphingomyelin (SM), cardiolipin (CL), and cholesterol (Chol).

Plasma membranes consist of fluid and semi-permeable bilayers, which are formed by different phospholipids (Figure S1). Each cell is surrounded by an outer cell wall that serves as a barrier, keeping important components within cells while blocking potentially harmful substances. Additionally, there are various organelles inside cells, which are responsible for the majority of cellular functions in biological systems. These organelles are enclosed by their own membranes, each with a unique lipid composition specific to the organelle's function (Table S1).

Table S1: Lipid distributions in various organelles.[3,4]

Membrane	**PM**	**OMM**	**IMM**	**ER**	**Golgi**	**LYS**
	% of total phospholipids (PL)					
Phosphatidylcholine	43	49	41	57	42	42
Phosphatidylethanolamine	21	34	38	21	21	21
Phosphatidylinositol	7	9	6	9	6	6
Phosphatidylserine	4	1	1	4	1	1
Cardiolipin	0	5	16	0	0	0
Sphingomyelin	23	2	2	5	12	16
Cholesterol/PL molar ratio	0.76	0.06	0.07	0.07	0.15	0.49
Internal pH	7.2	7.7 – 8.2	7.7 – 8.2	7.2	6.6	4.7

[3] J. E. Vance, *Traffic*, **2015**, *16*, 1–18.
[4] F.-X. Theillet, A. Binolfi, T. Frembgen-Kesner, K. Hingorani, M. Sarkar, C. Kyne, C. Li, P. B. Crowley, L. Gierasch, G. J. Pielak, A. H. Elcock, A. Gershenson, P. Selenko, *Chem. Rev.*, **2014**, *13*, 6661–6714.

4 Anion transport

4.1 General remarks and liposomes preparation

Chloroform stock solutions were created from lipids (Figure 1): POPC, POPE, PtdIns, PE, sphingomyelin, cholesterol, and stored at -20°C. The cardiolipin, stored in ethanol, was pipetted in a round bottom flask, evaporated on a rotary evaporator and stored overnight under high vacuum, before being dissolved in chloroform, and stored at -20°C. Specific amounts of lipids, corresponding to their respective molar percentages in organelle membranes (Table 1) or pure POPC, were pipetted from the stock solutions into a 10 mL round bottom flask. A chloroform solution was evaporated under reduced pressure and the lipids film was dried under a high vacuum for 8 or more hours. The lipids film was rehydrated by vortexing with 1 mL of internal solution which was first heated to 60°C before addition. The suspension was subjected to nine freeze-thaw cycles by freezing in a liquid nitrogen bath and thawing at a 60°C water bath. The lipid suspension was allowed to rest at 60°C for 30 min and extruded 25 times through a 200 nm polycarbonate membrane (Nucleopore TM) using an extruder set (Avanti Polar Lipids Inc) to form monodisperse vesicles. Elevated temperature during liposome preparation (60°C) enables work with phospholipids at the high transition temperature.

4.2 HPTS NMDG-Cl assay

Liposomes preparation

Liposomes were prepared as described in Section 4.1. Lipids film was hydrated with an aqueous solution of HPTS (1 mM, 100 mM NMDG-Cl and 10 mM HEPES, pH 7.0). Unencapsulated HPTS was removed by passing the mixture through a column with Sephadex using an aqueous solution of NMDG-Cl (100 mM, 10 mM HEPES, pH 7.0) as eluent. The collected vesicles were diluted with aqueous solution of NMDG-Cl (100 mM, 10 mM HEPES, pH 7.0) to reach the lipid concentration of 0.1 mM.

Measurement

A stock solution of squaramide **1** (5 mM), equivalent to 10 mol% of the vesicle concentration, was prepared in DMSO. Subsequent samples were generated by serial dilution of this stock solution.

Vesicle suspension (0.1 mM, 2.5 mL) was placed in a quartz cuvette with a small stirring bar and 5 µL of transporter **1**, specified at a certain molar percentage, was added to the cuvette. The fluorescence emission of the intravesicular HPTS was recorded using a fluorometer as a function of time. An NaOH pulse (25 µL, 0.5 M) was added to basify the external solution to pH 8.0 to initiate the start of the experiment. After t = 210 s a solution of Triton X-100 (11 w%) in DMSO:H_2O (1:7, v/v) (50 µL) was added to lyse the vesicles to fully dissipate the pH gradient and a final fluorescence reading was t = 300 s. DMSO control experiments were performed in the absence of the transporter, and experiments were independently repeated in triplicate.

HPTS was used as a ratiometric probe to measure the H^+/Cl^- symport (or equivalent OH^-/Cl^- antiport) through the intravesicular pH change during the experiment. The acidic and basic forms of HPTS were excited at λ_{ex} = 403 nm and λ_{ex} = 460 nm respectively, and the fluorescence emission of both forms was collected at λ_{em} = 510 nm. The fluorescence intensity ratio (R) of the basic form and the acidic form of HPTS was calculated, which allowed the calculation of the fractional fluorescence intensity (I_f) using Equation 1.

$$I_f = \frac{R_t - R_0}{R_d - R_0}$$

Equation 1. Calculation of the fractional fluorescence intensity (I_f) from the raw HPTS data.

Where R_t is the ratiometric fluorescence value at a given time (t), R_0 is the ratiometric fluorescence value at t = 0 s and R_d is the fluorescence ratiometric value recorded at t = 300 s following vesicular lysis.

Dose response experiments were performed with at least six different receptor concentrations providing varying percentage Cl^- efflux values at 200 s. The fractional fluorescence (I_f) was plotted as a function of the receptor concentration (mol %) and was fitted to the Hill equation using Origin2022:

$$y = y_0 + (y_{max} - y_0) \cdot \frac{x^n}{(k^n + x^n)}$$

Equation 2. The Hill equation.

Where y is the I_f at 200 s, y_0 is the I_f value at 200 s for the DMSO blank run, y_{max} is the maximum I_f value, x is the receptor concentration (mol %, with respect to lipid), n is the Hill coefficient (number of cooperative sites).

4.3 HPTS nonactin assay

Liposomes preparation

Chloroform solutions of POPC and 1 mol% of POPE were transferred into a 10 mL round bottom flask, and evaporated under reduced pressure. The lipids film was dried under a high vacuum for 8 or more hours. The lipids film was hydrated with an aqueous solution of HPTS (1 mM, 100 mM NaCl and 10 mM HEPES, pH 7.0). The suspension was subjected to nine freeze-thaw cycles by freezing in a liquid nitrogen bath and thawing at a 30°C water bath. The lipid suspension was allowed to rest for 30 min and extruded 25 times through a 200 nm polycarbonate membrane (Nucleopore TM) using an extruder set (Avanti Polar Lipids Inc) to form monodisperse vesicles. Unencapsulated HPTS was removed by passing the mixture through a column with Sephadex using an aqueous solution of NaCl (100 mM, 10 mM HEPES, pH 7.0) as eluent. The collected vesicles were diluted with aqueous solution of NaCl (100 mM, 10 mM HEPES, pH 7.0) to reach the lipid concentration of 0.1 mM.

Measurement

Vesicle suspension (0.1 mM, 2.5 mL) was placed in a quartz cuvette with a small stirring bar and 5 µL of POPE (1 mol%) was added to the cuvette (no incubation or 1 h incubation). The fluorescence emission of the intravesicular HPTS was recorded using a fluorometer as a function of time. Nonactin was added (0.1 mol%), followed by the addition of a NaOH pulse (25 µL, 0.5 M) to basify the external solution to pH 8.0, and to initiate the start of the experiment. After t = 210 s a solution of Triton X-100 (11 w%) in DMSO:H_2O (1:7, v/v) (50 µL) was added to lyse the vesicles to fully dissipate the pH gradient and a final fluorescence reading was t = 300 s. The acidic and basic forms of HPTS were excited at λ_{ex} = 403 nm and λ_{ex} = 460 nm respectively, and the fluorescence emission of both forms was collected at λ_{em} = 510 nm. The fluorescence intensity ratio (R) of the basic form and the acidic form of HPTS was

calculated, which allowed the calculation of the fractional fluorescence intensity (I_f) using Equation 1.

4.4 HPTS assay results

HPTS-based assay results and Hill analysis are shown for different vesicles.

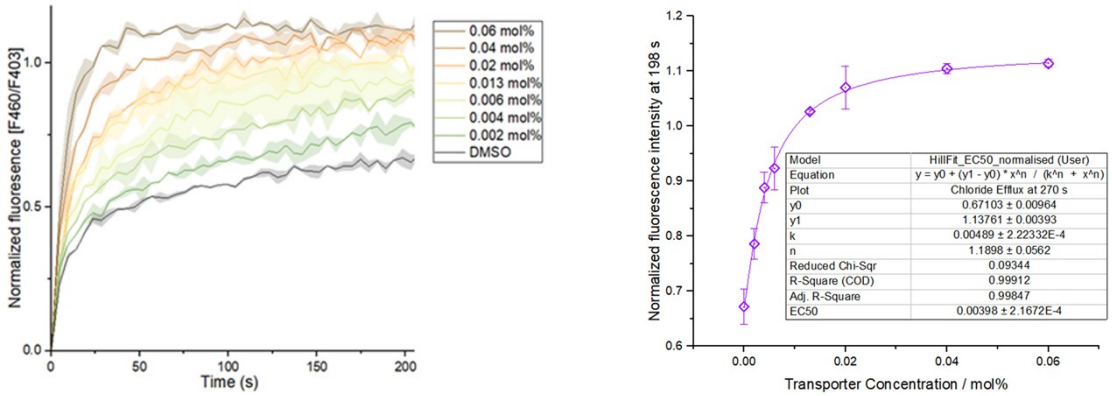

Figure S2. Left: the HPTS flux signal observed upon the addition of NaOH base pulse (0.5 M, 25 µL) to the external solution containing 0.1 mM vesicles, whose lipids composition mimicked plasma membrane (PM) and contains transporter **1** at various concentrations (mol% related to lipids). Right: Hill curves plotted from the HPTS flux values at 270 s and fitted using the Hill equation.

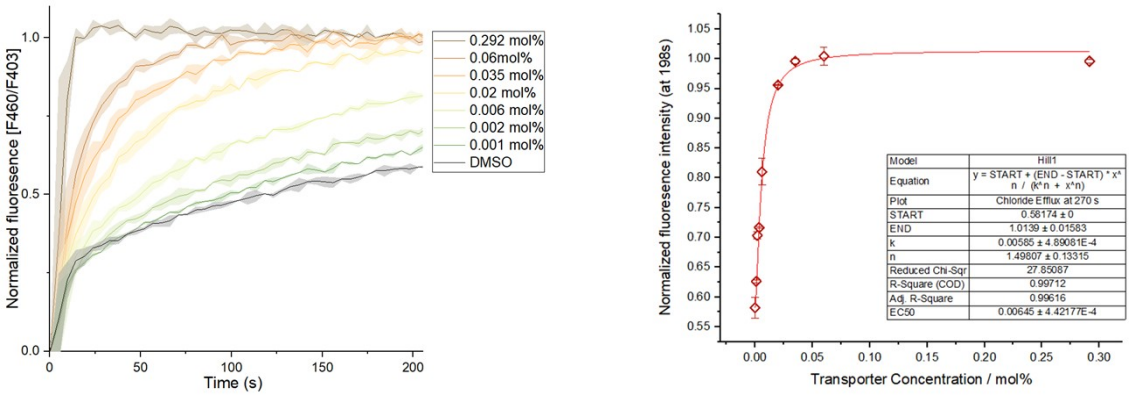

Figure S3. Left: the HPTS flux signal observed upon the addition of NaOH base pulse (0.5 M, 25 µL) to the external solution containing 0.1 mM vesicles, whose lipids composition mimicked outer mitochondrial membrane (OMM) and contains transporter **1** at various concentrations (mol% related to lipids). Right: Hill curves plotted from the HPTS flux values at 270 s and fitted using the Hill equation.

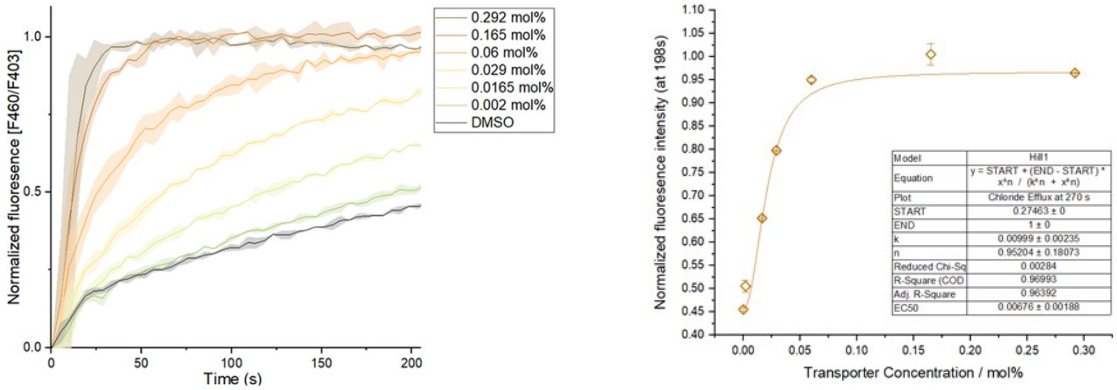

Figure S4. Left: the HPTS flux signal observed upon the addition of NaOH base pulse (0.5 M, 25 µL) to the external solution containing 0.1 mM vesicles, whose lipids composition mimicked inner mitochondrial membrane (IMM) and contains transporter **1** at various concentrations (mol% related to lipids). Right: Hill curves plotted from the HPTS flux values at 270 s and fitted using the Hill equation.

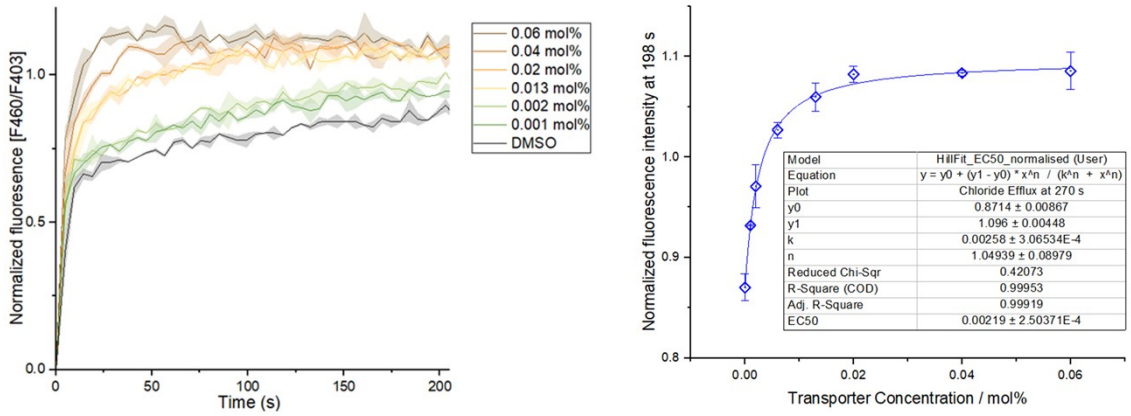

Figure S5. Left: the HPTS flux signal observed upon the addition of NaOH base pulse (0.5 M, 25 µL) to the external solution containing 0.1 mM vesicles, whose lipids composition endoplasmic reticulum membrane (ER) and contains transporter **1** at various concentrations (mol% related to lipids). Right: Hill curves plotted from the HPTS flux values at 270 s and fitted using the Hill equation.

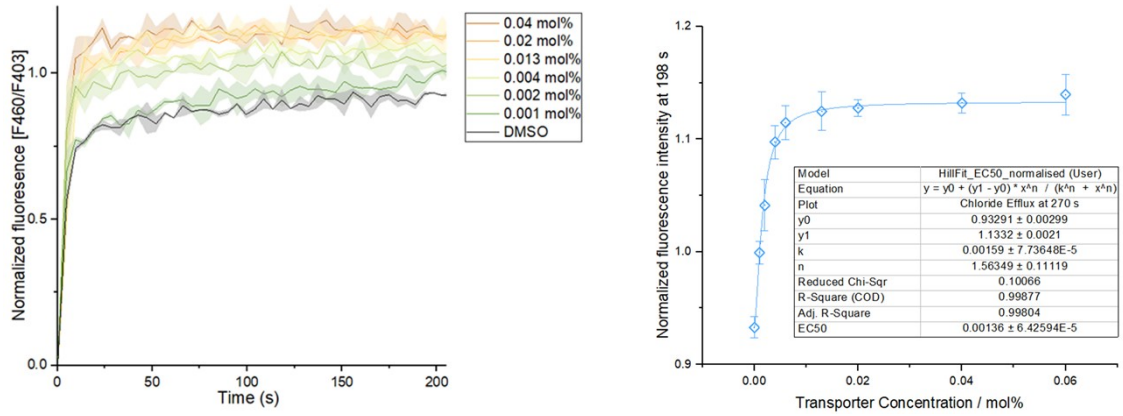

Figure S6. Left: the HPTS flux signal observed upon the addition of NaOH base pulse (0.5 M, 25 µL) to the external solution containing 0.1 mM vesicles, whose lipids composition mimicked Golgi apparatus membrane (Golgi) and contains transporter **1** at various concentrations (mol% related to lipids). Right: Hill curves plotted from the HPTS flux values at 270 s and fitted using the Hill equation.

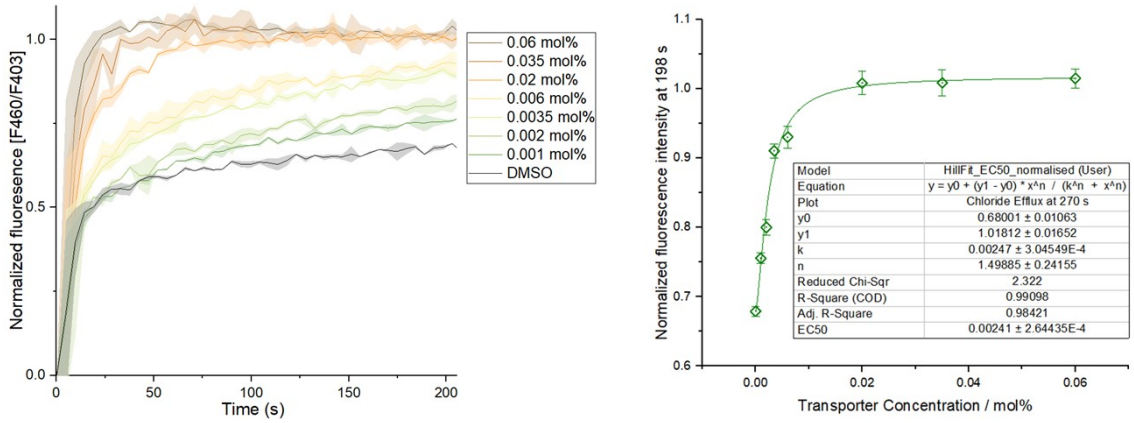

Figure S7. Left: the HPTS flux signal observed upon the addition of NaOH base pulse (0.5 M, 25 µL) to the external solution containing 0.1 mM vesicles, whose lipids composition mimicked lysosome membrane (LYS) and contains transporter **1** at various concentrations (mol% related to lipids). Right: Hill curves plotted from the HPTS flux values at 270 s and fitted using the Hill equation.

4.5 ISE-based assay

In ion-selective electrode (ISE) assay, only the internal solution of the vesicle contains chloride, while the external solution contains a large counter-ion (gluconate) that cannot interact with the lipid system. Upon addition of the transporter, H^+/Cl^- is transported out of the vesicle. Through addition of cationophore monensin, a natural K^+/H^+ antiporter, the extracted proton is reintroduced into the vesicle, making the process pH independent.

The ISE experiment was conducted using a Thermo Scientific Orion Star A211 pH meter, equipped with an ISE probe and a stirring plate, and controlled using a Star Com program.

The electrode was calibrated against NaCl solutions of known concentrations before each experiment in accordance with the supplier's manual. The electrode potential, y, was plotted against the respective concentration of NaCl, x, and fit to a simplified version of the Nernst equation (equation 6) in Origin2022 to afford the calibration parameters P_1 and P_2:

$$y = (P_1 log_{10} x) + P_2$$

Equation 6. The simplified Nernst equation.

Using equation 6, the chloride concentration can be calculated at any point during the experiments by using the calculated parameters P_1 and P_2, and the raw electrode value, y, to solve for x. Subtracting the Cl^- concentration at t_0 from the Cl^- concentration at any time point within the experiment ($t \geq 0$) provided the total Cl^- concentration released from the vesicles at any given time. The data was subsequently converted to percentage Cl^- efflux to allow for a simpler comparison. This conversion involved normalising that data using the 100% Cl^- efflux value recorded at the end of the experiment, t = 420 s, upon treatment of Triton X-100 (11 wt%) in H_2O:DMSO (7:1 v/v).

Liposomes preparation

Liposomes were prepared as described in Section 4.1. The lipids film was hydrated with an aqueous solution of KCl (300 mM, 10 mM HEPES, pH 7.0). To remove the excess chloride ions outside the vesicles, the vesicles undergo dialysis for 12 hours. Following dialysis, the lipid stock was diluted to 10 mL with the external solution to a known concentration. The lipid solution was further diluted with the external solution in a 10 mL glass vial to afford a test solution (1 mM, 5 mL).

Measurement

A stock solution of squaramide **1** (2.5 mM), equivalent to 0.5 mol% of the vesicle concentration, was prepared in DMSO. Subsequent samples were generated by serial dilution of this stock solution.

Cationophore monensin (0.5 mM) was prepared as a DMSO solution.

Vesicle suspension (1 mM, 5 mL) was placed in a plastic vial with a small stirring bar. Stirring was set to 600 rpm, and the solution was left to equilibrate until the reading from the ISE stabilized. 10 µL of monensin (0.5 mM, 0.1 mol%) was added to the vial, followed quickly by the addition of 10 µL of transporter **1** (2.5 mM). After 5 minutes, the vesicles are completely lysed through the addition of 50 µL triton-X detergent, to determine a normalization baseline. The measurement is continued for an additional 2 minutes. DMSO control experiments were performed in the absence of the transporter, and experiments were independently repeated in triplicate.

Data processing was done in OriginPro. Hill curves were plotted using the flux at 270 s for all relevant concentrations. A curve was fit using the Hill equation (equation 2).

4.6 ISE assay results

ISE-based assay results and Hill analysis are shown for different vesicles.

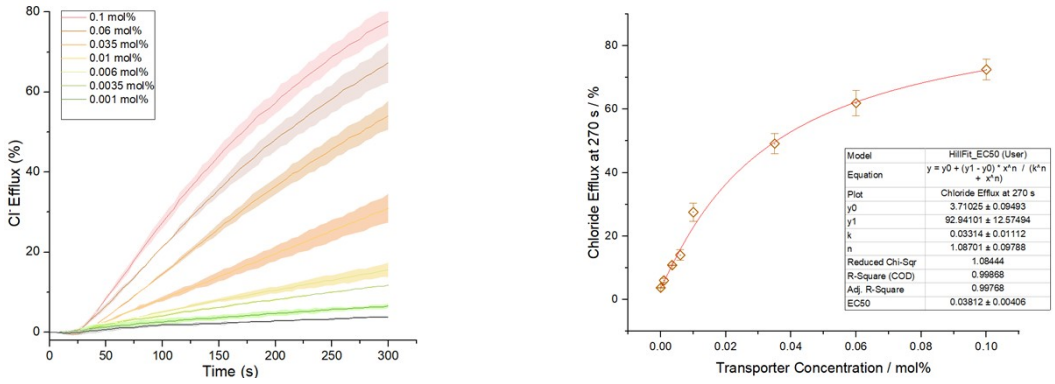

Figure S8. Left: the ISE flux signal observed upon the addition of 10 µL of monensin (0.5 mM) and 10 µL of transporter **1** at various concentrations to the external solution containing 1 mM vesicles, whose composition mimicked plasma membrane (PM). Right: Hill curves plotted from the ISE flux values at 270 s and fitted using the Hill equation.

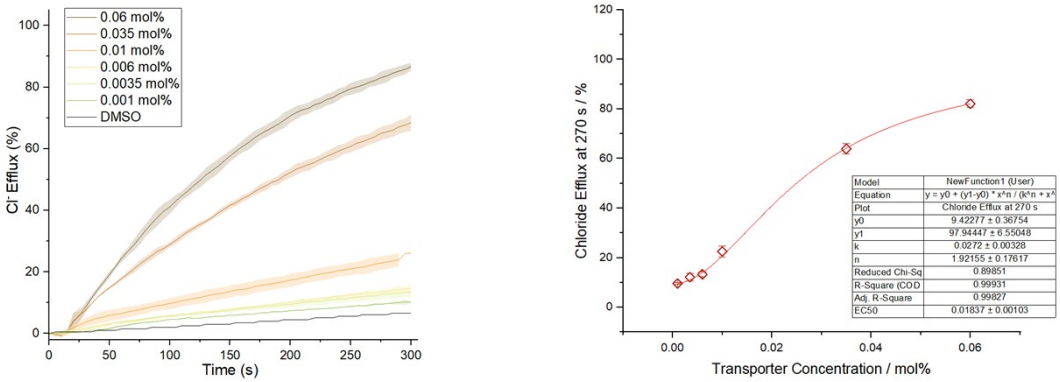

Figure S9. Left: the ISE flux signal observed upon the addition of 10 µL of monensin (0.5 mM) and 10 µL of transporter **1** at various concentrations to the external solution containing 1 mM vesicles, whose composition mimicked outer mitochondrial membrane (OMM). Right: Hill curves plotted from the ISE flux values at 270 s and fitted using the Hill equation.

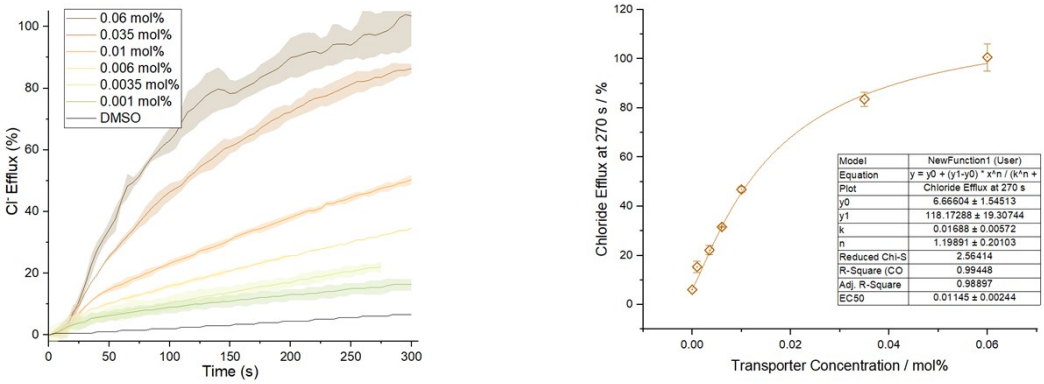

Figure S10. Left: the ISE flux signal observed upon the addition of 10 µL of monensin (0.5 mM) and 10 µL of transporter **1** at various concentrations to the external solution containing 1 mM vesicles, whose composition mimicked inner mitochondrial membrane (IMM). Right: Hill curves plotted from the ISE flux values at 270 s and fitted using the Hill equation.

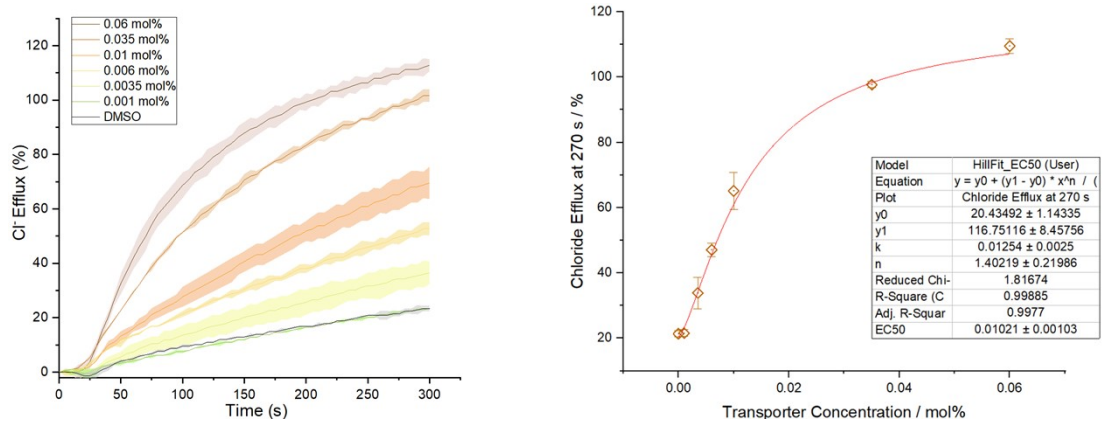

Figure S11. Left: the ISE flux signal observed upon the addition of 10 µL of monensin (0.5 mM) and 10 µL of transporter **1** at various concentrations to the external solution containing 1 mM vesicles, whose composition mimicked the endoplasmic reticulum (ER). Right: Hill curves plotted from the ISE flux values at 270 s and fitted using the Hill equation.

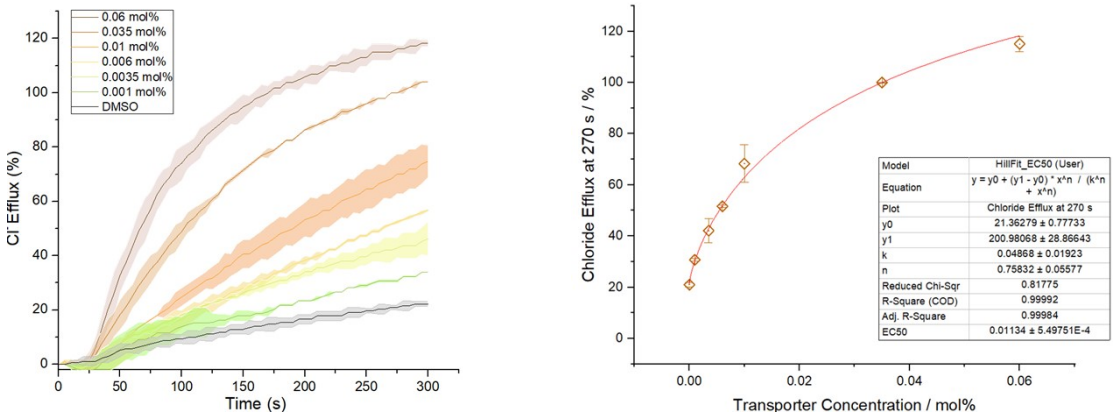

Figure S12. Left: the ISE flux signal observed upon the addition of 10 µL of monensin (0.5 mM) and 10 µL of transporter **1** at various concentrations to the external solution containing 1 mM vesicles, whose composition mimicked Golgi apparatus membrane (Golgi). Right: Hill curves plotted from the ISE flux values at 270 s and fitted using the Hill equation.

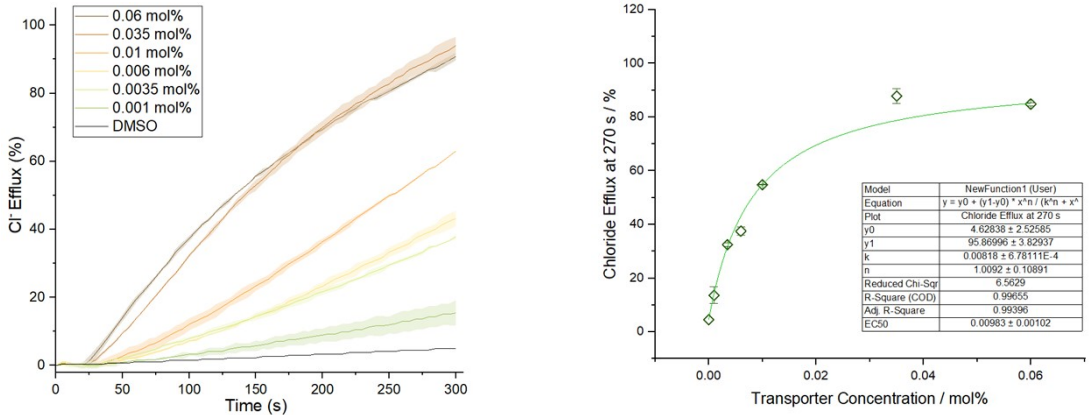

Figure S13. Left: the ISE flux signal observed upon the addition of 10 µL of monensin (0.5 mM) and 10 µL of transporter **1** at various concentrations to the external solution containing 1 mM vesicles, whose composition mimicked lysosome membrane (LYS). Right: Hill curves plotted from the ISE flux values at 270 s and fitted using the Hill equation.

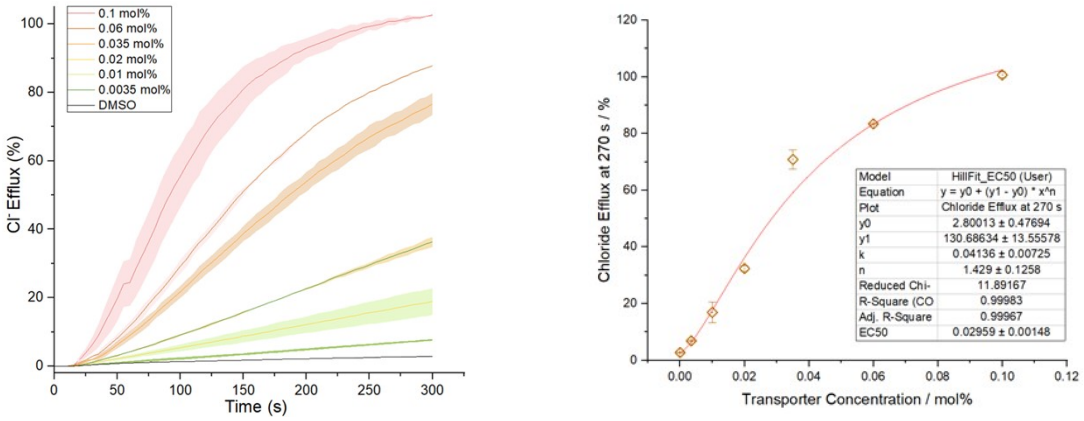

Figure S14. Left: the ISE flux signal observed upon the addition of 10 µL of monensin (0.5 mM) and 10 µL of transporter **1** at various concentrations to the external solution containing 1 mM POPC vesicles. Right: Hill curves plotted from the ISE flux values at 270 s and fitted using the Hill equation.

4.7 Difference in EC_{50} between subcellular vesicles types

Using the HPTS and ISE assay, a difference in EC_{50} values for the squaramide among the vesicle types was detected (Table S2).

Table S2. The determined EC_{50} for different vesicle types. The EC_{50} values for the HPTS assay are not trustworthy due to a competing POPE process, but are included for the sake of completion.

Model of membrane		**PM**	**OMM**	**IMM**	**ER**	**Golgi**	**LYS**
HPTS	EC_{50} (mol%)	0.0040±0.0002	0.0065±0.0004	0.0068±0.0019	0.0022±0.0003	0.0014±0.0001	0.0024±0.0003
	Hill coefficient	1.1898±0.0562	1.4981±0.1332	0.9520±0.1807	1.0494±0.0898	1.5635±0.1112	1.4989±0.2416
ISE	EC_{50} (mol%)	0.0381±0.0040	0.0184±0.0010	0.0112±0.0024	0.0102±0.0010	0.0113±0.0005	0.0098±0.0010
	Hill coefficient	1.0870±0.0979	1.9022±0.1762	1.1989±0.2010	1.4087±0.2199	0.7583±0.0558	1.0092±0.1089

4.8 Competitive deprotonation of HPTS by POPE

During the HPTS-based experiments, the expected increase in HPTS signal with increasing transporter concentration was observed (Section 4.3). However, upon the initiation of transport triggered by the addition of a NaOH base pulse (0.5 M, 25 µL) to the external solution, a notable surge in baseline intensity was noted, even in the absence of transporter (Figure S15). The increase in HPTS signal correlates directly with the deprotonation of the molecule. Given that our system contains few participants capable of deprotonating HPTS molecule, we hypothesised that phosphoethanolamine (POPE) emerges as the most probable deprotonating agent.

Indeed, we observe a prominent correlation between the quantity of POPE and the magnitude of the baseline deviation observed. Unlike the inner leaflet sequestration observed in natural systems, a portion of the POPE in our uniform-phase symmetric bilayers is exposed on the surface, making it susceptible to deprotonation by the applied base. Previous studies have demonstrated that the introduction of a pH gradient to model systems can lead to an asymmetric distribution of lipids across the inner and outer membrane leaflets. This mechanism relies on the concept that the uncharged form

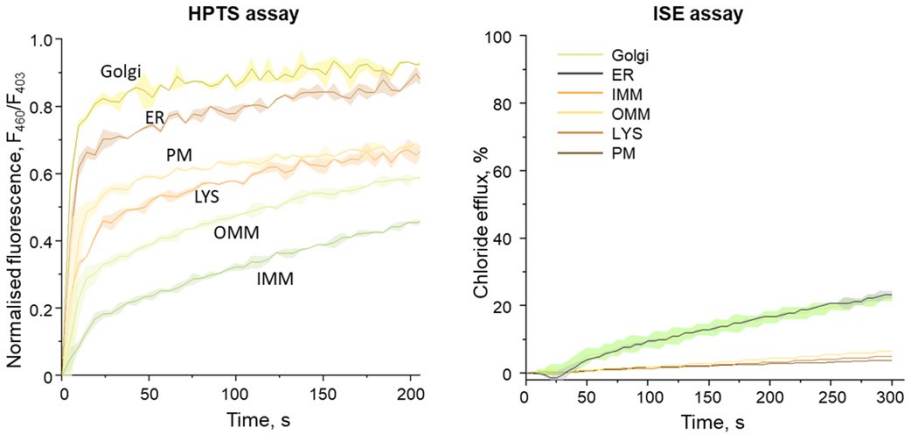

Figure S15. Left: HPTS signal observed upon the addition of NaOH (25 µL, 0.5 M) base pulse to the external solution containing 5 µL DMSO and 0.1 mM vesicles. Right: the ISE flux signal observed upon the addition of 10 µL of monensin (0.5 mM) and 10 µL of DMSO to the external solution containing 1 mM vesicles. Vesicle models of: Golgi apparatus (Golgi), endoplasmic reticulum (ER), plasma membrane (PM), lysosome (LYS), outer mitochondrial membrane (OMM), and inner mitochondrial membrane (IMM).

of a lipid undergoes translocation at a higher rate than its charged counterpart, resulting in an equilibrium dependent on the relative ionization state on either side of the lipid membrane.[5]

Here, we specifically examine spontaneous lipid transfer (SLT), also known as flip-flop, as natural lipid transporter proteins – floppases – are absent in our model systems. The rate of STL is highly dependent on experimental conditions and influenced by factors such as temperature, lipid crystallinity, leaflet composition, and species charge. POPE is a naturally zwitterionic molecule, containing both a negatively charged phosphate group and a positively charged ammonia group. Upon the introduction of the base, the ammonia group is deprotonated, resulting in a net negative charge on the lipid. In biology, it is often assumed that the spontaneous translocation of polar lipids is negligible, as it is believed to occur far too slowly on typical time scales. The time frame (<10s) in which the POPE translocation happens is thus quite surprising.

It has been shown that dispersion of headgroup polarity in POPC, through the addition of a low molecular weight synthetic translocase, can drastically increase flip-flop rate. These synthetic translocases function by forming hydrogen bonds with the headgroup of the lipid, effectively stabilizing part of the charge in the hydrophobic interior of the membrane.[6] Deprotonation of the ammonia headgroup of POPE may result in a similar occurrence. This, coupled with the introduced proton gradient, could realistically enhance the translocation rate into the inner membrane. Upon entering the inner membrane, POPE encounters the HPTS in the internal cavity which it promptly deprotonates, leading to an observed increase in HPTS ratio as detected by fluorescence. Subsequently, the transport out of the inner leaflet becomes significantly more unfavourable due to the restoration of its original charged headgroup state. The STL of the charged POPE lipid, referenced in the literature as having a half-time between 80 and 100 hours,[7] is negligible within the time frame of our experiment. As a result, the proton is unable to leave the inner leaflet, maintaining the charge distribution between the inside and outside of the vesicle.

[5] P. R. Cullis, M. J. Hope, M. B. Bally, T. D. Madden, L. D. Mayer and D. B. Fenske, *Biochim Biophys Acta.,* **1997**, *1331*, 187–211.
[6] J. M. Boon and B. D. Smith, *J. Am. Chem. Soc*., **1999**, *121*, 11924–11925.
[7] T. G. Pomorski and A. K. Menon, *Prog. Lipid Res*., **2016**, *64*, 69–84.

4.9 Lipid flip-flop from the perspective of energy barriers

Lipid flip-flop is a continuous process, with varying speeds ranging from seconds to days, depending on its favourability. The rate of lipid flip-flop is directly linked to the energy barrier associated with the process, as seen in transition state theory (equation 3).

$$k = \frac{K_B T}{h} \cdot exp\left(\frac{-\Delta G^{\ddagger}}{RT}\right)$$

Equation 3. Transition state theory.

Here we express the free energy of activation, or the energy barrier, as shown by Anglin et al.[8] Their work presents an expanded expression compared to Arrhenius theory, where the activation barrier is primarily assumed to be enthalpic, neglecting the entropic contribution. Anglin offer a more accurate description of the energy barrier, considering both enthalpic and entropic contributions (equation 4).

$$\Delta G^{\ddagger} = E_a - RT + \Pi \Delta a^{\ddagger} - T\Delta S^{\ddagger}$$

Equation 4. Anglin's equation.

In this context, E_a represents the activation energy according to Arrhenius's theory. $\Delta S^{\ddagger}$ denotes the entropy of activation, while $\Pi \Delta a^{\ddagger}$ is a two-dimensional work term relating to the area of activation and lateral surface pressure. Here the activation area ($\Delta a^{\ddagger}$) for STL describes the change in area occupied by a lipid when going from its original upright state, to the transition state in the lipid membrane. It is a direct indicator of how a localized expansion of the lipid bilayer is required to facilitate the transfer of each phospholipid across the membrane.[8] Lateral pressure (Π) refers to the pressure exerted by the lipids at the surface of the vesicle membrane in a lateral direction. It is directly related to the packing density of the lipids in the bilayer, thereby also reflecting on lipid size.[9] In considering the addition of POPE to the inner membrane, upon its re-protonation by HPTS, the significant energy barrier associated with the translocation of such a polar headgroup often results in the lipid effectively becoming trapped within the inner leaflet. Although the net charge is maintained, it becomes more concentrated at the lipid-water boundary compared to freely floating HPTS in the internal cavity. Additionally, a fundamental requirement requires the conservation of mass between the two bilayer leaflets. Thus, phospholipids crossing from one leaflet to the other must eventually be balanced by the transfer of a phospholipid in the opposite direction. Because the energy barrier is closely related to lateral membrane pressure (Π) and the area of activation ($\Delta a^{\ddagger}$), both of which depend on vesicle composition and asymmetric versus symmetric lipid distribution, each lipid flip effectively modulates the energy barrier.

As the extent of the reaction increases, defined as the ratio of $POPE_{in}$ to $POPE_{out}$, the energy barrier $\Delta G^{\ddagger}$ associated with a lipid transitioning from the outer membrane to its final state, accumulated on the inner leaflet, also increases. At a constant temperature, the rate of SLT is inversely proportional to the exponential of the free energy barrier (equation 3). **Therefore, as the energy barrier rises, the flipping rate decreases rapidly.** Therefore, here we see an inverse and counter-intuitive trend, where a larger POPE/POPC ratio (Table S3) results in a lower baseline (Figure S15).

[8] T. C. Anglin, M. P. Cooper, H. Li, K. Chandler and J. C. Conboy, *J. Phys. Chem. B,* **2010**, *114*, 1903–1914.
[9] T. C. Anglin and J. C. Conboy. *Biophys. J*, **2008**, *95*, 186–193.

Table S3. The ratio between POPE and POPC present in the various vesicle systems.

Model of membrane	PM	OMM	IMM	ER	Golgi	LYS
Phosphatidylcholine, %	43	49	41	57	42	42
Phosphatidylethanolamine, %	21	34	38	21	21	21
POPE/POPC ratio	0.488	0.694	0.927	0.368	0.500	0.500

This trend continues until the energy barrier $\Delta G^{\ddagger}$ equals that of the reverse reaction, at which point the rate of outward-to-inward flipping matches that of inward-to-outward flipping. At this point, protons from within the internal cavity of the vesicle would start to transport outward, eventually leading to the disappearance of the driving force, the pH gradient, over an extended period. However, due to the lengthy time-frame associated with this process and the limited duration of our measurements, we lack a comprehensive understanding of this regime.

4.10 Temperature influence of flip-flop rate

At the transition temperature (Tm), the lipid bilayer undergoes a phase change, transitioning from a more gel-like state to a liquid-crystal phase, where the passive flip-flop transition becomes greatly enhanced. The melting behavior of lipids in a vesicle system can vary significantly – with some systems exhibiting sharp "point-like" transitions and others displaying broader melting transitions – depending on the miscibility of the lipids involved.

In POPC/POPE mixtures, the transition temperature (Tm) diverges from the typical -2°C Tm observed for POPC lipids, depending on the amount of POPE (X_{POPE}) present.[10] Higher ratios of POPE lead to a shift in the Tm towards higher temperatures, reducing the presence of the liquid-crystal-like regime within our temperature range (between 22–25°C). In the OMM and IMM vesicles, this may lead to relatively ordered, gel-like vesicles where the majority of POPE exists in its crystalline state, making flip-flopping energetically unfavorable.[11,12] Therefore, we performed transport experiments in various temperatures to confirm this hypothesis. At elevated temperature, we observed an enhancement of the HPTS signal, which indicates an increased flip-flop rate of protonated POPE phospholipids (Figure S16).

[10] B. Eicher, D. Marquardt, F. A. Heberle, I. Letofsky-Papst, G. N. Rechberger, M.-S. Appavou, J. Katsaras, G. Pabst, *Biophys. J.*, **2018**, *114*, 146–157.
[11] D. Marquardt, F. A. Heberle, T. Miti, B. Eicher, E. Lomdon, J. Katsaras and G. Pabst, *Langmuir* **2017**, *33*, 3731–3741.
[12] J. S. Allhusen and J. C. Conboy, *Acc. Chem. Res*. **2017**, *50*, 58–65.

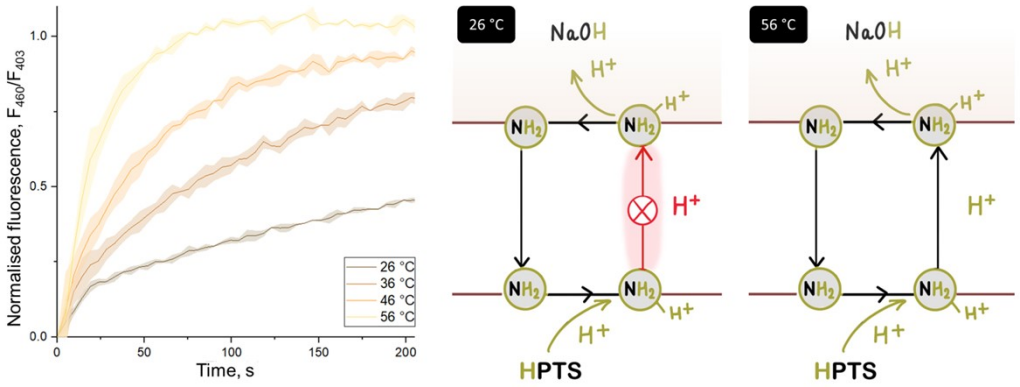

Figure S16. Left: the HPTS flux signal observed upon the addition of NaOH base pulse (0.5 M, 10 µL) to the external solution containing 5 µL DMSO and 0.1 mM vesicles, whose composition mimicked inner mitochondrial membrane (IMM) at various temperatures. Right: flip-flop of protonated POPE is faster in higher temperature.

4.11 Packing defects at domain boundaries

In biological systems, the combination of sphingomyelin and cholesterol has been observed to create a liquid-ordered domain referred to as a "lipid raft". Similarly, our mixture of unsaturated lipids can form vesicles with coexisting liquid-disordered, and, enriched in sphingomyelin and cholesterol, liquid-ordered domains (Figure S17).[13]

The presence of packing defects at membrane domain boundaries has been known to enhance spontaneous translocation rates.[14] This effect is hypothesized to arise from the relative stabilization of the transition state, where the phospholipid head is oriented towards the hydrophobic interior, due to pore formation.[11] Our vesicle model of Golgi membrane may contain an abundance of these boundaries, solely due to lipid composition. However, such boundary regions are also observed when a lipid mixture undergoes a phase transition. Although different, boundary regions between solid and gel domains have been proposed to exhibit a similarly increased permeability.[15] The combination of sphingomyelin and cholesterol may possess a lipophilicity uniquely suited to the squaramide transporter, resulting in increased partitioning of the transporter into these domains. This might be the reason for the facilitated transport leading to a lower overall EC_{50}.

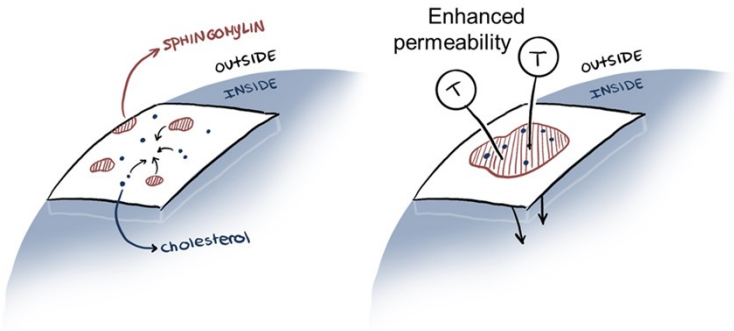

Figure S17. Graphical illustration of domain formation in the presence of sphingomyelin and cholesterol.

[13] P. Pathak and E. London. *Biophys. J.*, **2011**, *101*, 2417–2425.
[14] K. John, S. Schreiber, J. Kubelt, A. Herrmann and P. Müller, *Biophys. J.*, **2023**, *83*, 3315–3323.
[15] D. Papahadjopoulos, K. Jacobsoc, S. Nir and I. Isac, *Biochim. Biophys.* Acta, **1973**, *311*, 330–348.